Sensorless Speed Control of a 6-Phase Induction Machine using Adaptive Neural Fuzzy Inference Systems

M. Moghadasian, Franck Betin, Amine Yazidi

Available online www.jsaer.com

***Journal of Scientific and Engineering Research*, 2020, 7(7):170-179**

Research Article

ISSN: 2394-2630
CODEN(USA): JSERBR

Sensorless Speed Control of a 6-Phase Induction Machine using Adaptive Neural Fuzzy Inference Systems

M. Moghadasian[1,2], F. Betin[1], A. Yazidi[1]

[1]Laboratory of Innovative Technologies, University of Picardie "Jules Verne, Amiens, France
[2]Shohadaye Hoveyzeh University on Technology, Iran
franck.betin@u-picardie.fr

Abstract A new approach to the sensorless speed control of six-phase induction machine (6PIM) using an Adaptive Neural Fuzzy Inference Systems (ANFIS) as a rotor speed estimator to avoid mechanical sensor is proposed in this paper. The ANFIS is first trained offline to estimate the rotor speed in a wide range of operation and then implemented online to perform the field-oriented control (FOC) of the 6PIM. Fuzzy-PI (FPI) controllers are associated to FOC to control the rotor speed and the stator currents. For this, the input-output scale factors of the FPI systems are determined using Genetic Algorithms (GA). Experimental results assess the feasibility of the proposed method with high accuracy and good dynamic behavior in speed estimation and control of the 6PIM.

Keywords adaptive neural fuzzy inference systems (ANFIS), fuzzy-logic control, genetic algorithms, multiphase induction machine, real-time implementation, speed control

1. Introduction

Multiphase electric drives, dating back to 1969 [1], are nowadays considered as the best alternative for all applications requiring reliability and fault tolerance. Indeed, with a multiphase machine, the loss of one or more phases does not affect the drive since three phases are remaining to produce torque or power [2]. In this way, multiphase machines are often considered for high power applications such as automotive, aerospace, military and nuclear [3, 4]. Among the numerous possibilities of multiphase ac machines, the six-phase induction machine (6PIM) is probably the most popular in industrial applications.

Modern high-dynamic ac drives are equipped with a mechanical shaft sensor in order to estimate the flux position, which is required for field-oriented or direct torque control. Such sensor increases the drive cost, size, and maintenance requirements which decrease system reliability and robustness [5]. Different techniques for the speed-sensorless control of induction motors have been proposed in the literature during these last years [6]. However, parameter sensitivity, high computational effort, and stability at low and zero speeds can be the main shortcomings of sensorless control strategy [7] and recent research efforts are focused on extending the operating region of sensorless drives near zero stator frequency [8-11]. In this way, various control algorithms for eliminating the speed sensor have been proposed such as: algorithms using state equations [12], model reference adaptive systems [13], Luenberger- or Kalman-filter observers [14], saliency effects [15], sliding-mode controls [16], artificial intelligence [17], sensorless vector control [18], direct controls of torque and flux [19], nonlinear inverter model and parameter identification [20] and so on. These algorithms, which are mainly based on the flux and speed estimations obtained from the terminal electrical quantities, are really complicated and present some difficulties in the speed estimation.

Nevertheless, the designs of Soft computing tools such as Fuzzy Inference System (FIS), Artificial Neural

Networks (ANN) and Adaptive Neuro- Fuzzy Inference (ANFIS) do not need an exact mathematical model of the system and can be used in some power electronics applications, such as inverter current regulation [21], DC motor control [22], flux estimation [23], speed estimation [24] and observer-based control of induction machines [25]. The simple and less-intensive mathematical design requirements are the main features of intelligent systems, which are suitable to deal with nonlinearities and uncertainties of electric motors. However, a simple fuzzy-logic controller (FLC) has a narrow speed operation and needs much more manual adjustment by trial and error if high performance is desired. On the other hand, it is extremely tough to create a series of training data for ANNs that can handle all the operating modes [26], [27]. In this way, the concept of an ANFIS has emerged in recent years, as researchers have tried to combine the advantages of both FIS and ANN. The ANFIS uses the transparent linguistic representation of a fuzzy system with the learning ability of ANNs. Some of the advantages of ANFIS are the very fast convergence due to hybrid learning, and the ability to construct reasonably good input membership functions. The most striking feature of ANFIS is that it provides more choices over membership functions. It has more tracking ability and adaptability than the other controllers [28].
In this paper, an estimator of the rotor speed using ANFIS is associated to FOC with FPI controllers in such a way to control the speed of a 6PIM without requiring any speed sensor. The input and output scale factors of all FPI systems are tuned by genetic algorithms (GA) in order to minimize error of control variables. Section 1 is devoted to the modeling of the 6PIM used for simulation while Section 2 is dedicated to the estimation and control of the rotor speed using ANFIS and FPI regulators. Simulation tests are then presented in Section 4 to test feasibility of the proposed approach and the experimental results realized on a 90W 6PIM test bed show a high quality response and accurate performances of the proposed method in the estimation and control of the rotor speed for 6PIM.

2. Model of the 6PIM

It is well known that even for a three-phase induction machine, it is not easy to control the motor in the stationary reference frame. Therefore, it is necessary to transform the mathematical model of the system in a dq reference frame. In this way and in order to develop the model of the 6PIM in the dq reference frame, some assumptions have to be made beforehand. Hence, the windings are assumed to be sinusoidally distributed and the rotor cage is equivalent to a six-phase wound rotor. Furthermore, the magnetic saturation, the mutual leakage inductances and the core losses are neglected. Then, the electrical equations in the stationary reference frame for the stator and the rotor may be written as following [3, 4]:

$$[V_s] = [R_s][i_s] + p([L_{ss}][i_s] + [L_{sr}][i_r]) \quad (1)$$

$$0 = [R_r][i_r] + p([L_{rr}][i_r] + [L_{rs}][i_s]) \quad (2)$$

where

$$[V_s] = [v_a v_c v_b v_{a'} v_{c'} v_{b'}]^T \qquad [I_s] = [i_{as} i_{cs} i_{bs} i_{a's} i_{c's} i_{b's}]^T \qquad [I_r] = [i_{ar} i_{cr} i_{br} i_{a'r} i_{c'r} i_{b'r}]^T$$

Applying the transformation matrix [T_6], where $\gamma = \pi/3$, the 6PIM can be decomposed into three two-dimensional orthogonal subspaces: (α,β), (z1,z2) and (z3, z4) [1]. With this transformation, the 6PIM field oriented control (FOC) is similar to the classical 3PIM one. The components of the stator current in the rotating reference frame dq0 are obtained by applying the following transformation matrix:

$$[T_6] = \frac{1}{\sqrt{3}} \begin{bmatrix} 1 & \cos(\gamma) & -\frac{1}{2} & \cos(2\pi/3+\gamma) & -\frac{1}{2} & \cos(4\pi/3+\gamma) \\ 0 & \sin(\gamma) & \frac{\sqrt{3}}{2} & \sin(2\pi/3+\gamma) & -\frac{\sqrt{3}}{2} & \sin(4\pi/3+\gamma) \\ 1 & \cos(\pi-\gamma) & -\frac{1}{2} & \cos(\pi/3-\gamma) & -\frac{1}{2} & \cos(5\pi/3-\gamma) \\ 0 & \sin(\pi-\gamma) & -\frac{\sqrt{3}}{2} & \sin(\pi/3-\gamma) & \frac{\sqrt{3}}{2} & \sin(5\pi/3-\gamma) \\ 1 & 0 & 1 & 0 & 1 & 0 \\ 0 & 1 & 0 & 1 & 0 & 1 \end{bmatrix} \quad (3)$$

$$[T_2]=\begin{bmatrix}\cos(\lambda) & \sin(\lambda)\\ -\sin(\lambda) & \cos(\lambda)\end{bmatrix} \tag{4}$$

By assuming that the quadratic component is equal to zero on the contrary of the direct component, it leads to the basic FOC equation $\varphi = \varphi_r = \varphi_{dr}$. Consequently, after these transformations, the 6PIM equations in a rotating reference frame can be written as:

$$\begin{cases} v_{ds} = \sigma L_s \frac{di_{ds}}{dt} + \left(R_s + R_r \frac{M^2}{L_r^2}\right) i_{ds} - \sigma L_s \omega i_{qs} - \frac{M}{T_r L_r}\phi \\ v_{qs} = \sigma L_s \frac{di_{qs}}{dt} + \left(R_s + R_r \frac{M^2}{L_r^2}\right) i_{qs} - \sigma L_s \omega i_{ds} - \frac{M}{T_r L_r}\omega_r \phi \\ J\frac{d\omega_r}{dt} = \frac{M}{L_r} i_{qs}\phi - F\omega_r - T_L \\ \frac{d\phi}{dt} = -\frac{1}{T_r}\phi + \frac{M}{T_r} i_{ds} \end{cases} \tag{5}$$

$$\text{where} \begin{cases} \sigma = 1 - \frac{M^2}{L_s L_r} \\ T_r = \frac{L_r}{R_r} \end{cases} \tag{6}$$

3. Speed Controller and Estimator Design

Fig. 1 shows the proposed control scheme with the matrix transformations, the decoupling terms, the current control loops, the speed control loop and the ANFIS speed estimation block. The proposed Fuzzy -PI (FPI) regulators have been introduced in the inner (current) and the outer (speed) loops to regulate i_{qs}, and i_{ds} and ω. Indeed, the outer controller works on error of ω and calculates i_{qs}^* while the inner ones regulate i_{qs} (resp. i_{ds}) and calculate v_{qs} (resp. v_{ds}).

In the sensorless speed control of induction motors with direct field orientation, the rotor flux and speed informations are given by the observers. However, the exact values of the parameters that build the observers are difficult to measure and changeable with respect to the operating conditions. ANFIS speed estimation algorithm can be used to estimate the motor speed in real time without a speed sensor. This algorithm needs two stator current and voltage signals and employs DSP techniques to filter and manipulate the speed-related harmonics.

3.1. Fuzzy -PI Speed Controller

A typical FPI controller scheme is shown in Fig. 2. Since the fuzzy controller is basically an input/output static nonlinear mapping, the controller action can be written as

$$dU = \alpha E + \beta dE/dt \tag{7}$$

where α and β are nonlinear coefficients or gain factors. Integrating both sides results in equation:

$$U = \alpha \int E dt + \beta E \tag{8}$$

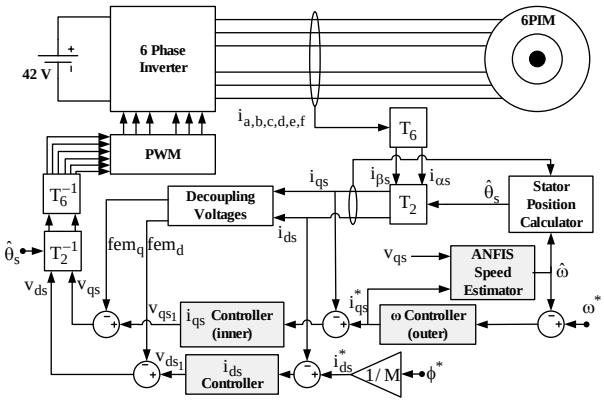

Figure 1: General control scheme

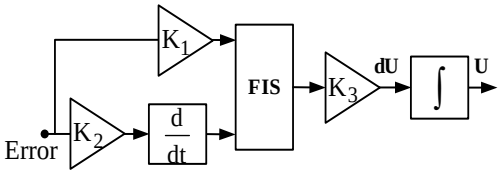

Figure 2: Fuzzy-PI (FPI) controller scheme

The basic FLC block is composed of fuzzification interface, fuzzy rules with inference mechanism, and defuzzification interface. The input/output variables are fuzzified by seven triangular membership functions (MF) normalized on the universe of discourse between −1 and +1 (NB—negative big, NM—negative medium, NS—negative small, ZE—zero, PS—positive small, PM—positive medium, and PB—positive big) as shown in Fig. 3. The fuzzy rule matrix are very close to Mac Vicar Whelan rules [4] associated with the Max–Min inference method. These rules were designed based on the dynamic behavior of the error signal, resulting in the symmetrical matrix. The output signal of the FLC is computed by center of gravity method. The input and output scale factors of the FPI controllers (K_1, K_2, K_3 in Fig. 2) are tuned using an off-line genetic algorithm (GA) system to minimize the ω, i_{qs}, i_{ds} errors. The fitness function used to evaluate the individuals of each generation has been chosen as integral with time of absolute error (ITAE):

$$\mathrm{ITAE} = \int_0^t t\,|\,E(t)\,|\,dt \qquad (9)$$

During the search process, the GA looks for the optimal setting of the FPI controller gains which minimize the cost function. Individuals with low ITAE are considered as the fittest. Each chromosome represents a solution of the problem and hence it consists of three genes composing the chromosome vector [K_1, K_2, K_3]. The genetic algorithm parameters chosen for the FPI tuning purpose are shown in Table 1.

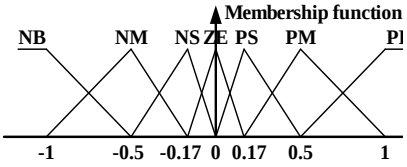

Figure 3 : MF used in FPI controllers

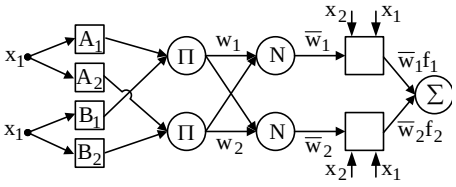

Figure 4: ANFIS structure

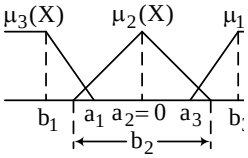

Figure 5: MF for ANFIS

Table 1: Genetic Algorithm Parameters to Determine FPI Controllers' Scaling Factors

Number of generations	50
Number of chromosomes in each generation	30
Number of genes in each chromosome	3
Chromosome length	24 bit
Crossover method	single-point
Crossover probability & Mutation rate	0.7 & 0.05

3.2. ANFIS Speed Estimator

The ANFIS has proven to be an excellent function approximation tool [30]. Fig. 4 shows a typical ANFIS structure with two inputs (x_1 and x_2) and one output (f) with a first-order Sugeno-style fuzzy system as:

Rule i: if x is A_i and y is B_i, then $f_i = p_i x + q_i y + r_i$ (10)

where A_i and B_i are the fuzzy sets in the antecedent while p_i, q_i, and r_i are the design parameters that are determined during the training process. As in Fig. 4, the ANFIS network is formed with five layers:

Layer 1: This layer is also known as fuzzification one, where each node is represented by a square. Here, three membership functions are assigned to each input. The trapezoidal and triangular membership functions are employed to reduce the computation burden, as shown in Fig. 5. The value of parameters {a_i, b_i} changes according to the error, and accordingly generates the linguistic value of each membership function. Parameters in this layer are referred as *premise parameters* or *precondition parameters*.

Layer 2: Every node in this layer is a circle labeled as Π, which multiplies the incoming signals and forwards it to the next layer. Here, the output of each node represents the firing strength of a rule.

Layer 3: Every node in this layer is represented as a circle. This layer calculates the normalized firing strength of each rule.

Layer 4: Every node in this layer is a square node with a node function given in [29].

Layer 5: This layer is also called output layer, which computes the output. The output from this layer are now multiplied with the normalizing factor and passed through the low-pass filter to find the estimated value of the rotor speed of the 6PIM.

Due to high dependency of the rotor speed to q-axis stator current (i_{qs}) and voltage (v_{qs}), it can be estimated using an adaptive neural fuzzy inference system (ANFIS) as shown in Fig. 4. From Speed-i_{qs} and Speed-v_{qs} data obtained from the motor operated in different speed phases, 60 data groups are obtained. Data used in training are given in Table 2.

4. Simulation Results

The effectiveness of the proposed scheme is validated by a MATLAB/Simulink program developed to model the whole system shown in Fig. 1. Simulation and experimental tests are performed on a 90-W inverter-duty induction motor, with parameters summarized in Table III. Prior to testing the control approach, the reference model performance is confirmed by considering the response of the model to a step change in reference speed, shown in Fig. 6. The ability of the proposed algorithm to reject load disturbance was simulated at 400 rpm reference speeds with 50% of nominal load. Fig. 7 shows the simulation of 6PIM speed response to a trapezoidal speed reference without load torque. The real and estimated percentage of speed error (11) is shown in the second row of the Fig. 7:

$$E_{\omega_{real(est.)}}(\%) = \frac{\omega^* - \omega_{real(est.)}}{\omega^*} \times 100 \qquad (11)$$

Table 2: Data Used For Training of ANFIS

i_q^*	v_q	$\omega_{(rpm)}$	i_q^*	v_q	$\omega_{(rpm)}$
0.003	0.002	10	0.083	0.075	310
0.005	0.005	20	0.085	0.077	320
0.008	0.007	30	0.088	0.080	330
0.011	0.010	40	0.091	0.082	340
0.013	0.012	50	0.093	0.084	350
0.016	0.015	60	0.096	0.087	360
0.018	0.017	70	0.099	0.090	370
0.020	0.020	80	0.100	0.092	380
0.024	0.022	90	0.104	0.094	390
0.027	0.024	100	0.107	0.096	400
0.029	0.027	110	0.109	0.099	410
0.032	0.029	120	0.112	0.101	420
0.035	0.031	130	0.115	0.104	430
0.037	0.033	140	0.117	0.106	440
0.040	0.036	150	0.120	0.109	450
0.043	0.039	160	0.123	0.111	460
0.045	0.040	170	0.125	0.113	470
0.048	0.043	180	0.128	0.116	480
0.050	0.046	190	0.131	0.118	490
0.053	0.048	200	0.133	0.121	500
0.056	0.050	210	0.136	0.123	510
0.059	0.053	220	0.138	0.125	520
0.061	0.055	230	0.141	0.128	530

0.064	0.058	240	0.144	0.130	540
0.067	0.060	250	0.146	0.133	550
0.069	0.063	260	0.149	0.135	560
0.072	0.065	270	0.152	0.137	570
0.075	0.068	280	0.154	0.140	580
0.077	0.070	290	0.157	0.142	590
0.080	0.072	300	0.160	0.145	600

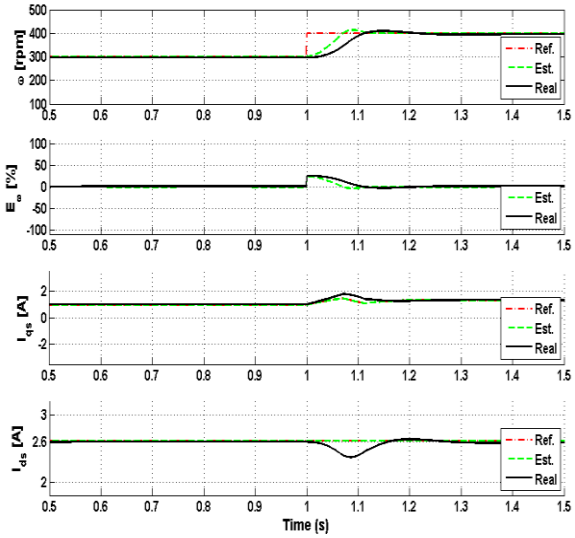

Figure 6: Simulation results of step speed response of the 6PIM at 50% of nominal load

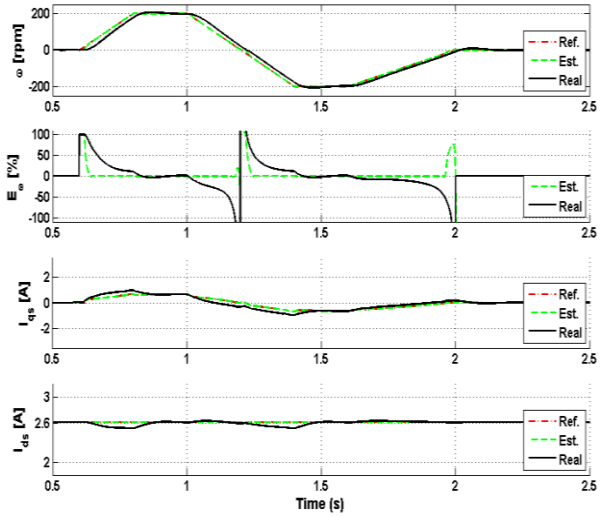

Figure 7: Simulation results of speed response of the 6PIM to a sequence of the speed steps

The steady state error of the estimated and actual speed is negligible which shows the effectiveness of the proposed method. The third and fourth rows show performances of the FPI controller and the ANFIS estimator in control of i_{qs} and i_{ds}.

5. Experimental Results

The experimental setup has been developed as shown in Fig. 8. Our test bed is composed of a 6PIM supplied by two three-phase voltage source inverters with MOSFET as power switches whose dc link voltage is 42 V. The switching frequency is set at 10 kHz using the classical sampled natural PWM technique generated by an FPGA. The digital control board has been built around an Intel-Pentium 4 processor allowing easily an actual sampling period of 100µs. This board receives the stator current data through six 12-bit A/D converters with a maximum

frequency of 20 kHz and the dc bus voltage with a frequency of 12.8 kHz. Figs. 9-10 show the experimental results of the same speed reference profiles introduced in the previous section. As it can be seen in the Fig. 10, the actual and estimated experimental speed error is very low, just as for simulation results.

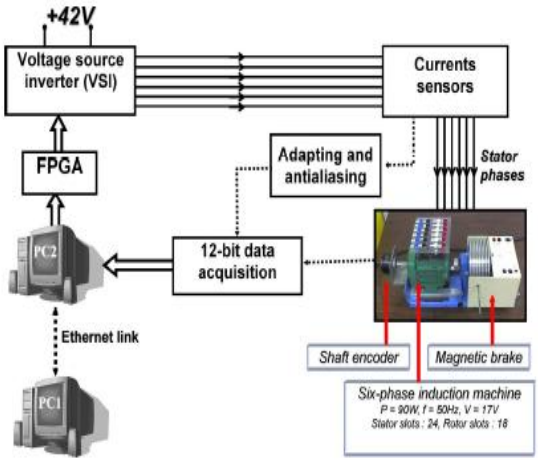

Figure 8: The exprimental setup

Table 3: 6PIM Parameters

Rated power	90 W
Rated torque	0.3 N.m
VSI DC source	42 V
No. of poles	2
Mutual inductance	30.9 mH
Stator resistance	1.04 Ω
Stator leakage inductance	0.3 mH
Rotor resistance	0.64 Ω
Rotor leakage inductance	0.65 mH
Friction coefficient	4×10^{-4} N.m/rd/s
Inertia coefficient (J)	9.5×10^{-5} Kg.m^2

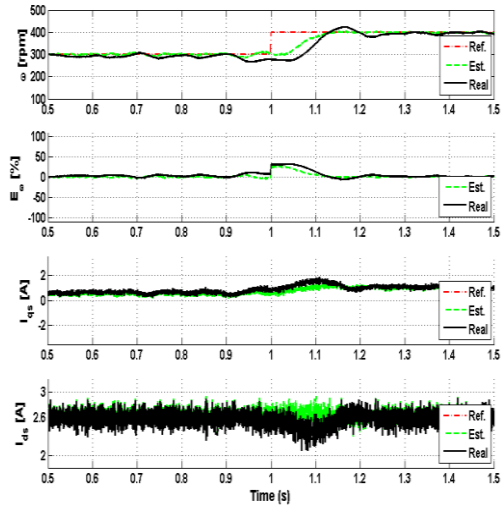

Figure 9: Experimental results of step speed response of the 6PIM at 50% of nominal load

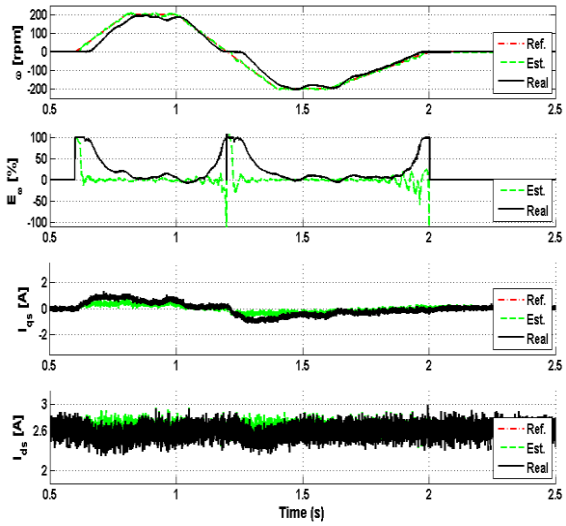

Figure 10: Experimental results of speed response of the 6PIM to a sequence of the speed steps

6. Conclusion

In this paper, an intelligent sensorless control algorithm has been implemented in order to obtain a high-precision speed estimation and control for six-phase induction machine (6PIM) using Adaptive Neuro- Fuzzy Inference (ANFIS) and Fuzzy-PI (FPI) controller tuned by Genetic and low computational effort in real-time implementation. Numerical and real-time implementation of the novel Algorithm (GA). The advantages of the proposed scheme are a minimum number of parameters to be offline optimized, robustness to parameters uncertainties and noise, smooth operation at low speed and load speed reversal and stability at zero speed.

References

[1]. E.E. Ward and H. Härer, Preliminary investigation of an invertor-fed 5-phase induction motor, Proc. IEE 116 (1969) (6), pp. 980–984.

[2]. M.A. Abbas, R. Christen and T.M. Jahns, Six-phase voltage source inverter driven induction motor, IEEE Trans. Ind. App. IA-20 (1984).

[3]. R. Kianinezhad, B. Nahid-Mobarakeh, L. Baghli, F. Betin, G.A. Capolino, Modeling and Control of Six-Phase Symmetrical Induction Machine Under Fault Condition Due to Open Phases, IEEE Trans. Ind. Elec., Vol. 55, No. 5, May 2008, pp 1966-1977.

[4]. M.A. Fnaiech, F. Betin, G.A. Capolino, F. Fnaiech, Fuzzy logic and sliding-mode controls applied to six-phase induction machine with open phases, IEEE Trans. Ind. Elec., Vol. 57, No. 1, JAN. 2010.

[5]. T. M. Wolbank, M. A. Vogelsberger, R. Stumberger, S. Mohagheghi, T. G. Habetler and R. G. Harley, Autonomous Self-Commissioning Method for Speed-Sensorless-Controlled Induction Machines, IEEE Trans. Ind. App., Vol. 46, No. 3, May/June 2010.

[6]. N. Salvatore, A. Caponio, F. Neri, S. Stasi, and G. L. Cascella, Optimization of Delayed-State Kalman-Filter-Based Algorithm via Differential Evolution for Sensorless Control of Induction Motors, IEEE Trans. Ind. Elec., Vol. 57, No. 1, Jan 2010.

[7]. S. M. Gadoue, D. Giaouris and J. W. Finch, Sensorless Control of Induction Motor Drives at Very Low and Zero Speeds Using Neural Network Flux Observers, IEEE Trans. Ind. Elec., Aug 2009.

[8]. J. Holtz and J. Quan, Drift and parameter compensated flux estimator for persistent zero stator frequency operation of sensorless controlled induction motors, IEEE Trans. Ind. Appl., Jul./Aug. 2003.

[9]. M. Rashed and A. F. Stronach, A stable back-EMF MRAS-based sensorless low speed induction motor drive insensitive to stator resistance variation, IEEE Proc. Inst. Elect., Nov., 2004.

[10]. C. Caruana, G. M. Asher, K. J. Bradley, and M. Woolfson, Flux position estimation in cage induction machines using synchronous HF injection and Kalman filtering, IEEE IAS Annu. Meeting, 2002.

[11]. C. Caruana, G. M. Asher, and J. Claire, Sensorless vector control at low and zero frequency considering zero-sequence current in Delta connected cage induction motors, IEEE IECON, 2003.
[12]. Beres Z, Vranka P. Sensorless IFOC of induction motor with current regulators in current reference frame. IEEE Trans Ind Appl 2001; 37: 1012–8.
[13]. Vasic V, Vukosavic S. Robust MRAS-based algorithm for stator resistance and rotor speed identification. IEEE Power Eng Rev 2001.
[14]. Ritter CM, Silvino JL. An alternative sensorless field orientation method. IEEE Trans Energy Convers 1999; 14: 1335–40.
[15]. Ha JI, Ohto M, Jang JH, Sul SK. Design and selection of AC machines for saliency-based sensorless control. _In: Conf rec IEEE-IAS annu meeting; 2002. p. 1155–62.
[16]. Li J, Xu L, Zhang Z. An adaptive sliding-mode observer for induction motor sensorless speed control. IEEE Trans Ind Appl 2005; 41(4).
[17]. Campbell J, Sumner M. Practical sensorless induction motor drive employing an artificial neural network for online parameter adaptation. Proc IEE—Elect Power Appl 2002; 149(4):255–60.
[18]. Edelbaher G, Jezernik K, Urlep E. Low-speed sensorless control of induction machine. IEEE Trans Ind Electron 2005; 53(1):120–9.
[19]. Maes J, Melkebeek J. Speed sensorless direct torque control of induction motors using an adaptive flux observer. _In: Conf rec IEEE-IAS annu meeting; 1999. p. 2305–12.
[20]. Joachim H, Quan J. Sensorless vector control of induction motors a very low speed using a nonlinear inverter model and parameter identification. IEEE Trans on Ind Appl 2002;38(4):1087–95.
[21]. Burton B, Harley RG, Habetler TG. High bandwidth direct adaptive neurocontrol of induction motor current and speed using continual online random weight change training. In: PESC 99. 30th ann. IEEE power electronics specialists conference, vol. 1(27); 1999. p. 488–94.
[22]. Herrmann G, Ge SS, Guoxiao G. Practical implementation of a neural network controller in a hard disk drive. IEEE Trans Control Syst Technol 2005; 13(1):146–54.
[23]. Cirrincione M, Pucci M, Cirrincione G, Capolino GA. A new adaptive integration methodology for estimating flux in induction machine drives. IEEE Trans Power Electron 2004; 19(1): 25–34.
[24]. Tsai C-H. CMAC-based speed estimation method for sensorless vector control of induction motor drive. Electr Power Compon Syst 2006; 34: 1213–30.
[25]. Y. Oguz, M. Dede, Speed estimation of vector controlled squirrel cage asynchronous motor with artificial neural networks, Energy Conversion and Management 52 (2011) 675–686.
[26]. Y. Chen, B. Yang, X. Gu, and S. Xing, Novel fuzzy control strategy of IPMSM drive system with voltage booster, in Proc. 6th World Congr. Intell. Control Autom., Jun. 21–23, 2006, vol. 2.
[27]. Y. Yi, D. M. Vilathgamuwa, and M. A. Rahman, Implementation of an artificial-neural-network based real-time adaptive controller for an interior permanent-magnet motor drive, IEEE Trans. Ind. Appl., vol. 39, no. 1, pp. 96–104, Jan./Feb. 2003.
[28]. Md. M. I. Chy, and M. N. Uddin, Development and Implementation of a New Adaptive Intelligent Speed Controller for IPMSM Drive, IEEE Trans. Ind. App., Vol. 45, No. 3, May/June 2009.
[29]. M. Singh, and A. Chandra, Application of Adaptive Network-Based Fuzzy Inference System for Sensorless Control of PMSG-Based Wind Turbine with Nonlinear-Load-Compensation Capabilities, IEEE Pow. Elec., Vol. 26, No. 1, Jan 2009.
[30]. J. S. R. Jang, "ANFIS: Adaptive-network-based fuzzy inference systems," IEEE Syst., Man, Cybern. C, vol. 23, no. 3, May 1993.

Nomenclature

‖X‖	Euclidean norm of vector X
^{T}	Transpose of vector X
v	Instantaneous phase voltage
i	Instantaneous phase current
Φ	Linkage flux

R	Resistance
L	Inductance
M	Mutual inductance
J	Total shaft inertia
F	Friction coefficient
T	Electromagnetic torque
ω_s	Stator MMF angular speed
ω	Rotor electrical angular speed (rpm)
P	Number of pole pares
s	Stator quantities
r	Rotor quantities
d	Direct axis component
q	Quadrature axis component
P	Derivative operator
X^*	Reference value of variable X
γ	Phase shift between two consecutive stator windings
θ	Flux position